JOURNAL OF VIROLOGY, June 2009, p. 6087–6097 Vol. 83, No. 12
0022-538X/09/$08.00+0 doi:10.1128/JVI.00160-09
Copyright © 2009, American Society for Microbiology. All Rights Reserved.

Bovine Coronavirus Nonstructural Protein 1 (p28) Is an RNA Binding Protein That Binds Terminal Genomic *cis*-Replication Elements▽

Kortney M. Gustin,[1] Bo-Jhih Guan,[1] Agnieszka Dziduszko,[2] and David A. Brian[1,2]*

Departments of Microbiology[1] and Pathobiology[2], University of Tennessee College of Veterinary Medicine, Knoxville, Tennessee 37996-0845

Received 23 January 2009/Accepted 29 March 2009

Nonstructural protein 1 (nsp1), a 28-kDa protein in the bovine coronavirus (BCoV) and closely related mouse hepatitis coronavirus, is the first protein cleaved from the open reading frame 1 (ORF 1) polyprotein product of genome translation. Recently, a 30-nucleotide (nt) *cis*-replication stem-loop VI (SLVI) has been mapped at nt 101 to 130 within a 288-nt 5′-terminal segment of the 738-nt nsp1 cistron in a BCoV defective interfering (DI) RNA. Since a similar nsp1 coding region appears in all characterized groups 1 and 2 coronavirus DI RNAs and must be translated in *cis* for BCoV DI RNA replication, we hypothesized that nsp1 might regulate ORF 1 expression by binding this intra-nsp1 cistronic element. Here, we (i) establish by mutation analysis that the 72-nt intracistronic SLV immediately upstream of SLVI is also a DI RNA *cis*-replication signal, (ii) show by gel shift and UV-cross-linking analyses that cellular proteins of ~60 and 100 kDa, but not viral proteins, bind SLV and SLVI, (SLV-VI) and (iii) demonstrate by gel shift analysis that nsp1 purified from *Escherichia coli* does not bind SLV-VI but does bind three 5′ untranslated region (UTR)- and one 3′ UTR-located *cis*-replication SLs. Notably, nsp1 specifically binds SLIII and its flanking sequences in the 5′ UTR with ~2.5 μM affinity. Additionally, under conditions enabling expression of nsp1 from DI RNA-encoded subgenomic mRNA, DI RNA levels were greatly reduced, but there was only a slight transient reduction in viral RNA levels. These results together indicate that nsp1 is an RNA-binding protein that may function to regulate viral genome translation or replication but not by binding SLV-VI within its own coding region.

Coronaviruses (CoVs) (59) cause primarily respiratory and gastroenteric diseases in birds and mammals (35, 71). In humans, they most commonly cause mild upper respiratory disease, but the recently discovered human CoVs (HCoVs), HCoV-NL63 (65), HCoV-HKU1 (73), and severe acute respiratory syndrome (SARS)-CoV (40) cause serious diseases in the upper and lower respiratory tracts. The SARS-CoV causes pneumonia with an accompanying high (~10%) mortality rate (69). The ~30-kb positive-strand CoV genome, the largest known among RNA viruses, is 5′ capped and 3′ polyadenylated and replicates in the cytoplasm (41). As with other characterized cytoplasmically replicating positive-strand RNA viruses (3), translation of the CoV genome is an early step in replication, and terminally located *cis*-acting RNA signals regulate translation and direct genome replication (41). How these happen mechanistically in CoVs is only beginning to be understood.

In the highly studied group 2 mouse hepatitis coronavirus model (MHV A59 strain) and its close relative the bovine CoV (BCoV Mebus strain), five higher-order *cis*-replication signals have been identified in the 5′ and 3′ untranslated regions (UTRs). These include two in the 5′ UTR required for BCoV defective interfering (DI) RNA replication (Fig. 1A) described as stem-loop III (SLIII) (50) and SLIV (51). Recently, the SLI region in BCoV (15) has been reanalyzed along with the homologous region in MHV and is now described as comprising SL1 and SL2 (Fig. 1A), of which SL2 has been shown to be a *cis*-replication structure in the context of the MHV genome (38). In the 3′ UTR, two higher-order *cis*-replication structures have been identified that function in both DI RNA and the MHV genome. These are a 5′-proximal bulged SL and adjacent pseudoknot that potentially act together as a unit (23, 27, 28, 72) and a 3′-proximal octamer-associated bulged SL (39, 76) (Fig. 1A). In addition, the 5′-terminal 65-nucleotide (nt) leader and the 3′-terminal poly(A) tail have been shown to be *cis*-replication signals for BCoV DI RNA (15, 60).

In CoVs, the 5′-proximal open reading frame (ORF) of ~20 kb (called ORF 1) comprising the 5′ two-thirds of the genome is translated to overlapping polyproteins of ~500 and ~700 kDa, named pp1a and pp1ab (41). pp1ab is formed by a −1 ribosomal frameshift event at the ORF1a-ORF1b junction during translation (41). pp1a and pp1ab are proteolytically processed into potentially 16 nonstructural protein (nsp) end products or partial end products that are proposed to function together as the replicase (24). ORF 1a encodes nsps 1 to 11 which include papain-like proteases (nsp3), a 3C-like main protease (nsp5), membrane-anchoring proteins (nsps 4 and 6), a potential primase (nsp8), and RNA-binding proteins (nsp 7/nsp 8 complex and nsps 9 and 10) of imprecisely understood function (19, 20, 24, 25, 29, 43, 49, 77). ORF 1b encodes nsps 12 to 16 which function as an RNA-dependent RNA polymerase, a helicase, an exonuclease, an endonuclease, and a 2′-*O*-methyltransferase, respectively (6, 17, 24, 44). 3′ Proximal genomic ORFs encoding structural and accessory proteins are translated from a 3′-nested set of subgenomic mRNAs (sgmRNAs) (41).

* Corresponding author. Mailing address: Department of Microbiology, University of Tennessee, Knoxville, TN 37996-0845. Phone: (865) 974-4030. Fax: (865) 974-4007. E-mail: dbrian@utk.edu.

▽ Published ahead of print on 8 April 2009.

Downloaded from http://jvi.asm.org/ on March 29, 2015 by ST ANDREWS UNIV

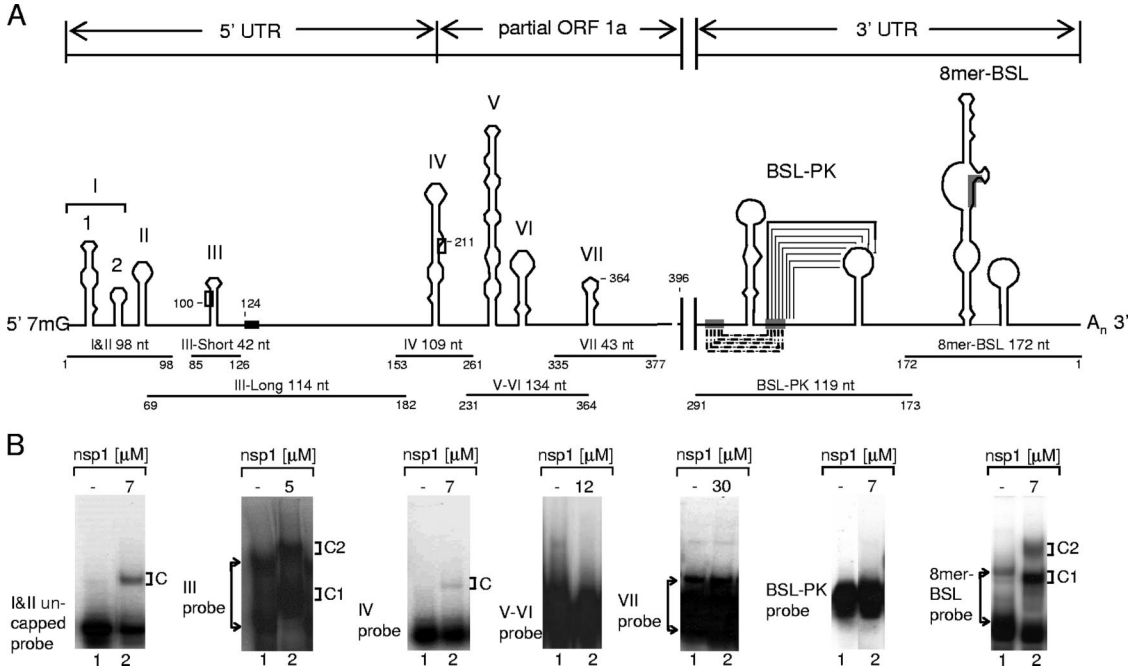

FIG. 1. RNA structures in the BCoV genome tested for nsp1 binding. (A) BCoV 5′-terminal and 3′-terminal *cis*-acting RNA SL structures and flanking sequences identified for BCoV DI RNA replication. Regions of the genome are identified and SL *cis*-replication elements are identified schematically. Open boxes at nt 100 and 211 identify AUG start codons for the short upstream ORF and ORF 1, respectively. A closed box at nt 124 identifies the UAG stop codon for the short upstream ORF. Shown below the SL structures are the RNA segments used as ^{32}P-labeled probes in the gel shift assays. BSL-PK, bulged SL-pseudoknot; 8mer-BSL, octamer-associated bulged SL. (B) Gel shift assays for probes when used with purified nsp1. Protein-RNA complexes identifying a shifted probe are labeled C.

The N-terminal ORF 1a protein, nsp1, in the case of BCoV and MHV is also named p28 to identify the cleaved 28-kDa product (18). The precise role of nsp1 in virus replication has not been determined, but it is known that a sequence encoding an N-proximal nsp1 region in MHV (nt 255 to 369 in the 738-nt coding sequence) cannot be deleted from the genome without loss of productive infection (10). nsp1 also directly binds nsp7 and nsp10 (11) and by confocal microscopy is found associated with the membranous replication complex (10, 66) and virus assembly sites (11). The amino acid sequence of nsp1 is poorly conserved among CoVs, indicating that it may be a protein that interacts with cellular components (1, 58). In the absence of other viral proteins, MHV nsp1 induces general host mRNA degradation (79) and cell cycle arrest (16). The SARS-CoV nsp1 homolog, a 20-kDa protein, has been reported to cause mRNA degradation (30, 45), inhibition of host protein synthesis (30, 45, 70), inhibition of interferon signaling (70, 79), and cytokine dysregulation in lung cells (36).

In this study, we examine the RNA-binding properties of BCoV nsp1 with the hypothesis that it is a potential regulator of translation or replication through its binding of SLVI mapping within its coding region. The rationale for this hypothesis stems from five observations. (i) In the BCoV DI RNA, the 5′-terminal one-third (approximately) of the nsp1 cistron and the entire nucleocapsid (N) protein cistron together comprise the single contiguous ORF in the DI RNA, and most of both coding regions appear required for DI RNA replication (15). (ii) The partial nsp1 cistron in the DI RNA must be translated in *cis* for DI RNA replication in helper virus-infected cells (12, 14). (iii) A similar part of the nsp1 cistron is found in the genome of all characterized naturally occurring group 1 and 2 CoV DI RNAs described to date (7, 8). (iv) A *cis*-acting SL named SLVI is found within the partial nsp1 cistron in the BCoV DI RNA (12). (v) Translation, which involves a 5′→3′ transit of ribosomes, and negative-strand synthesis, which involves a 3′→5′ transit of the RNA-dependent RNA polymerase, cannot simultaneously occur on the same molecule with a single ORF (4, 31). Thus, to enable genome replication an inhibition of translation at least early in infection for cytoplasmically replicating positive-strand RNA viruses is required (4, 5, 22, 32). Mechanisms of translation inhibition have been described for the Qβ viral genome, wherein the viral replicase autoregulates translation by binding an intracistronic *cis*-replication element (32), and for the polio virus genome, wherein genome circularization inhibits the early translation step (5, 22). Therefore, since nsp1 is synthesized early and also contains an intracistronic *cis*-replication element, we postulated that it is autoregulatory with RNA binding properties.

Here, we do the following: (i) demonstrate by mutagenesis analysis that the 72-nt SLV, mapping immediately upstream of SLVI and within the partial nsp1 cistron, is also a *cis*-acting DI RNA replication element; (ii) show by gel shift and UV cross-linking analyses that there is likely no binding of an intracellular viral protein to SLV and SLVI (SLV-VI), but there is binding of unidentified cellular proteins of ~60 and 100 kDa; and (iii) show by gel shift analysis that recom-

Downloaded from http://jvi.asm.org/ on March 29, 2015 by ST ANDREWS UNIV

TABLE 1. Oligonucleotides used in this study

Oligonucleotide[a]	Polarity[b]	Sequence (5′→3′)[c]	Binding region in pDrep1 (nt)[d]
pRight-5′ 306/309	+	GGATAACCCTAG**C**AG**C**TCAGAGGT	294–317
pRight-3′ 306/309	−	ACCTCTGA**G**CT**G**CTAGGGTTATCC	294–317
pLeft-5′ 240/243	+	TCGA**G**CT**G**CACTGGGCTCCAGAATTTCC	236–263
pLeft-3′ 240/243	−	GGAAATTCTGGAGCCCAGTG**C**AG**C**TCGA	236–263
pRtLt-5′	+	CTCGA**G**CT**G**CACTGGGCTCCAGAATTTCC**C**TGGATG	235–270
pRtLt-3′	−	CATCCA**G**GGAAATTCTGGAGCCCAGTG**C**AG**C**TCGAG	235–270
pRtLt (−loops)-5′	+	AGAATTTCCATGGATGTTTGAGGACGCAGA	255–284
pRtLt (−loops)-3′	−	TCTGCGTCCTCAAACATCCATGGAAATTCT	255–284
pLoops-5′	+	CCAGAATTTCCCTGGATGTT**C**GAA**G**ACGCA	253–282
pLoops-3′	−	TGCGTCTTC**G**AACATCCA**G**GGAAATTCTGG	253–282
pRtLoops-L-5′	+	CACTGGGCTCCAGAATTTCC**C**TGGATG	244–270
pRtLoops-L-3′	−	CATCCA**G**GGAAATTCTGGAGCCCAGTG	244–270
pRtLoops-R-5′	+	GTT**C**GAA**G**ACGCAGAGGAGAAGTTGGATAACCCTAG**C**AG**C**TCA	270–312
pRtLoops-R-3′	−	TGA**G**CT**G**CTAGGGTTATCCAACTTCTCCTCTGCGTCTTC**G**AAC	270–312
150-HpaI-5′	+	GTTAACAGCTTTCAGCCAGGGACGTGTTG	150–178
600-XbaI-3′	−	TCTAGATTGGTCGGACTGATCGGCC	576–600
BCoV leader	+	GATTGTGAGCG	1–11
TGEV8(+)	−	CATGGCACCATCCTTGGCAACCCAGA	1098–1123
HSVgD(+)	−	GAGAGAGGCATCCGCCAAGGCATATTTG	1854–1885
3′UTR (+)	−	CAGCAAGACATCCATTCTGATAGAGAGTG	2226–2254

[a] The positive and negative symbols in the oligonucleotide names indicate the polarity of the nucleic acids to which the oligonucleotides anneal.
[b] Polarity of the oligonucleotide relative to the positive-strand DI RNA.
[c] Boldface nucleotides represent mutations.
[d] For probe binding to negative-strand sequence, the numbers correspond to complementary positive-strand sequence.

binant nsp1 purified from *Escherichia coli* does not bind SLV-VI but does bind SLs I to IV in the 5′ UTR and also the 3′-terminal bulged SL in the 3′ UTR, suggesting a possible regulatory role at these sites. Notably, specific binding with ~2.5 μM affinity of nsp1 to SLIII and its flanking regions in the 5′ UTR was observed. Additionally, we show that, under conditions that would express nsp1 from a DI RNA-encoded sgmRNA, DI RNA levels are greatly reduced; viral RNA species levels, however, are reduced only slightly, and this reduction is transient. These results together indicate that nsp1 is an RNA-binding protein that may function as a regulator of viral translation or replication but not through its binding of *cis*-acting SLs V and VI within its own cistron.

MATERIALS AND METHODS

Cells and viruses. A DI RNA-free stock of the Mebus strain of BCoV (GenBank accession number U00735) at 4.5×10^8 PFU/ml (14, 15) was grown on human rectal tumor cell line HRT-18 (64) as described previously (15). Other genome sequences analyzed were those of MHV-A59 (GenBank accession number NC_001846) and SARS-CoV-Toronto (GenBank accession number NL_004718).

RNA structure predictions. Mfold (http://mfold.bioinfo.rpi.edu/) (42, 78) was used to predict RNA secondary structures.

Plasmid constructs. To make BCoV DI RNA with mutations in SLV, PCR mutagenesis (52) was done using pDrep1 DNA. pDrep1 is a pGEM3Zf(−) (Promega)-based plasmid containing a cDNA clone of a naturally occurring 2.2-kb DI RNA of BCoV modified to carry a 30-nt in-frame reporter (15). For mutagenesis, overlapping primers bordering SLV and containing the desired base changes (Table 1) and HpaI and XbaI sites (occurring in pDrep 1 at nt 150 and 595, respectively) were used for directional ligation into wt pDrep1.

To make BCoV DI RNA for expressing wild-type (wt) nsp1 from subgenomic mRNAs, a modification of pDrep12.7 (75), which is itself a modification of pDrep1 (75), was used and named pDrep-ISnsp1. For this, a 756-nt fragment containing the upstream 7-nt template-switching core and flanking sequences for N mRNA (AATAATCTAAACTTTAAGG, a total of 18 nt called the intergenic sequence [IS]) (34) and the nsp1 cistron (BCoV genomic nt 211 to 948, a total of 738 nt) flanked by BamHI and KpnI restriction enzyme sites was used to replace the 198-nt BamHIKpnI fragment (nt 1667 to 1865) in pDrep12.7. For pDrep-ISnsp1$^{1–95}$, genomic nt 211 to 495 (encoding nsp1 amino acids[aa] 1 to 95) were used in place of the full-length nsp1 cistron to make the construct, and for pDrep-ISnsp1$^{95–246}$, genomic nt 493 to 948 (encoding nsp1 aa 95 to 246) were used.

To make RNA probes for gel shift analyses, primers bordering the *cis*-replication elements in pDrep 1 were used that had incorporated EcoRI and HindIII sites for directional ligation into EcoRI/HindIII-linearized pGEM3Zf(−) (Promega).

To make nsp1 in *E. coli*, the nsp1 cistron from BCoV (nt 211 to 948) was subcloned with BamHI and EcoRI site-containing primers into the BamHI/EcoRI site of pET28a(+) vector (Novagen). This construct yielded BCoV nsp1 with a 33-nt upstream His_6-thrombin site-T7 tag-encoding sequence.

RNA synthesis. For synthesis of uncapped positive-strand transcripts of SLV DI RNA mutants for testing mutational effects on DI RNA replication, 2 μg of MluI-linearized plasmid DNA was transcribed in a 100-μl reaction mixture containing 40 U of T7 RNA polymerase (Promega) following the Promega protocol for synthesis of uncapped nonlabeled RNA. The mix was treated with 3 U of RQ1 RNase-free DNase (Promega), and RNA was purified by silica matrix affinity using an RNaid kit (MP Biochemicals) and quantified spectrophotometrically.

For synthesis of positive-strand radiolabeled RNA probes, 2 μg of HindIII-linearized plasmid DNA was transcribed in a 50-μl reaction mixture containing 40 U of T7 RNA polymerase (Promega) and 120 μCi of [α^{32}P]UTP (3,000 Ci/mmole) (MP Biochemicals). The mixture was treated with 3 U of RQ1 RNase-free DNase (Promega), and probes were purified by electrophoresis on a 5 or 9% polyacrylamide–7% urea gel. RNA visualized by autoradiography was eluted from the excised gel band overnight in elution buffer (1 mM EDTA, 0.5 M ammonium acetate), and ethanol precipitated. Cerenkov counts were determined by scintillation counting in water.

Northern assay for DI RNA replication. Northern blot assays for detecting reporter-containing DI RNAs were performed essentially as described previously (56, 75). Briefly, cells ($\sim 6 \times 10^6$) at ~80% confluence in a 35-mm dish were infected with BCoV at a multiplicity of 10 PFU per cell and transfected 1 h later with 500 ng of RNA using Lipofectin (Invitrogen). At the indicated times postinfection, RNA was extracted with Trizol (Invitrogen) and stored in water at −20°C. For passage of progeny virus, supernatant fluids were harvested at 48 h postinfection (hpi), and 300 μl was used to infect freshly confluent cells ($\sim 8 \times 10^6$) in a 35-mm dish (called virus passage 1 [VP1]) from which supernatant fluids at 48 hpi were used to infect new cells (called VP2). For VP1 and VP2, RNA was extracted at 48 hpi. For electrophoretic

Downloaded from http://jvi.asm.org/ on March 29, 2015 by ST ANDREWS UNIV

resolution in a formaldehyde-agarose gel, one-quarter of the RNA from each dish was used per lane (where total RNA in dishes increased with time due to continued cell proliferation and one-quarter was ~14, 30, and 44 μg for 1, 24, and 48 hpi and ~100 μg each for VP1 and VP2). Approximately 1 ng of RNA transcript, identified as RNA in the Northern blot figures, was used as a marker. RNA was transferred to Hybond N^+ nylon membrane (Amersham) by vacuum blotting, and membranes were UV irradiated. Blots were probed with 20 pmol of γ-^{32}P-end-labeled oligonucleotide probe at ~5×10^5 cpm/pmol. The probes used were TGEV8(+) or HSVgD(+) (where TGEV is transmissible gastroenteritis virus and HSV is herpes simplex virus) for detecting DI RNA progeny and 3′UTR(+) for detecting DI RNA, viral genome, and viral sgmRNAs. Probed blots were exposed to Kodak XAR-5 film for 1 to 7 days at −80°C for imaging, and counts were quantified with a PhosphorImager (Molecular Dynamics).

Sequence analysis of progeny from mutant DI RNA replicons. Reverse transcription with Superscript II Reverse Transcriptase (Invitrogen) was done on RNA extracted at VP1 and VP2, and PCR was done with primers BCoV leader(−) and TGEV(+). PCR products were sequenced directly.

In vitro translation. A total of 500 ng of wt or mutant DI RNA as transcripts from plasmids was translated in a 50-μl reaction mixture of rabbit reticulocyte lysate (Promega) containing 20 μCi of [^{35}S]Met. At 90 min, proteins in a 5-μl sample were resolved by sodium dodecyl sulfate-polyacrylamide gel electrophoresis (SDS-PAGE) in a gel of 12% polyacrylamide, and radioactivity was quantified on the dried gel by phosphor imaging.

Cell lysate preparation. BCoV-infected and mock-infected cell lysates were prepared essentially as described by Thomson et al. (63). Briefly, cells from a 75-cm^2 flask were collected by scraping, and pelleted cells were resuspended in 100 μl of lysis buffer (10 mM HEPES [pH 7.5], 3 mM $MgCl_2$, 14 mM KCl, 5% glycerol, 0.5% NP-40, 1 mM dithiothreitol, 1× complete protease inhibitor [Roche]) and incubated on ice for 20 min. Lysates were clarified by microcentrifugation at 3,000 rpm for 4 min at 4°C, and aliquots were stored at −80°C. For infected cell lysates, cells were infected with at a multiplicity of infection of 10 viruses per cell, and lysates were prepared at 6 hpi. Protein concentrations were determined by the Bradford assay.

Protein expression and purification from *E. coli*. BL21(DE3) *E. coli* cells transformed with p28(+)-nsp1 were grown in LB medium containing 34 μg/ml chloramphenicol and 25 μg/ml kanamycin until an optical density at 600 nm of ~0.6. Protein expression was induced with 1 mM IPTG (isopropyl-β-D-thiogalactopyranoside), and cells were grown for an additional 15 h at 15°C. Cells (~10 g) were pelleted at 5,000 × *g*, flash frozen in liquid N_2, and resuspended with sonication in 30 ml of lysis buffer (50 mM Tris [pH 8.0], 0.3 M NaCl, 10 mM imidazole, 5% glycerol, 1 mM β-mercaptoethanol, 1 mM phenylmethylsulfonyl fluoride, 1× EDTA-free complete protease inhibitor [Roche], and 25 U/ml benzonase endonuclease [Novagen]). Fusion protein was purified by chromatography on Ni-nitrilotriacetic acid superflow resin (Qiagen), and nsp1 was released in column by thrombin cleavage and concentrated by filtration on YM-10 Centriprep/Centricons cellulose membranes (Millipore).

Gel shift assays. The method of Andino et al. (2) as modified by Silvera et al. (57) and as described here was used. Briefly, ~4×10^4 cpm of α-^{32}P-labeled RNA probe (1 to 5 ng) was incubated in a 15-μl binding reaction mixture containing 5 mM HEPES (pH 7.9), 40 mM KCl, 2 mM $MgCl_2$, 4% glycerol, 2 mM dithiothreitol, 0.25 μg/μl heparin, 1 U/μl RNasin (Promega), 0.5 μg/μl yeast tRNA, 1× EDTA-free complete protease inhibitor (Roche), and either 20 μg of HRT cell lysate protein, or purified *E. coli*-expressed fusion protein to make a final concentration of 5 to 30 μM. The mixture was preincubated without probe for 10 min at 30°C and then for an additional 10 min after probe was added. Two microliters of 50% glycerol was added, and reaction products were electrophoretically separated on a 5% nondenaturing polyacrylamide gel for approximately 4 h at 4°C. Gels were dried and exposed to Kodak XAR-5 film, and results were visualized by autoradiography and quantified by phosphor imaging.

UV cross-linking. The UV cross-linking method essentially as described by Pestova et al. (48) was used. Briefly, ~3×10^5 cpm of α-^{32}P-labeled RNA probe in 15 μl of binding reaction mixture with cell lysate was incubated as described for the gel shift assay and irradiated on ice at 3 mW/cm^2 for 30 min using a UV Stratalinker 1800. Irradiated reaction mixtures were treated with 2.5 U of RNase A, 100 U of RNase T_1, and 0.1 U of RNase CV1 (all from Ambion) for 30 min at 37°C, and proteins were resolved by SDS-PAGE. Dried gels were exposed to Kodak XAR-5 film for autoradiography.

Bioinformatics. Potential RNA and protein binding domains in BCoV and MHV nsp1 were predicted with the SMART program (http://smart.embl-heidelberg.de/) (37, 53). Sequence alignments were made with Vector NTI Suite 8 (Invitrogen).

RESULTS

SLV mapping within the nsp1 cistron immediately upstream of SLVI is a required *cis*-acting signal for DI RNA replication. A 30-nt SL, SLVI, mapping at nt 101 to 130 within the 5′-terminal partial nsp1 cistron (genomic nt 311 to 340) (Fig. 1A and 2A) was recently identified as a *cis*-acting replication element for BCoV DI RNA (12). Although its *cis*-replication feature remains to be tested in the context of the full-length viral genome, this SL along with the frame-shifting pseudoknot at the ORF 1a/1ab junction (9) are, to our knowledge, the only higher-order *cis*-replication elements known within CoV ORF 1 (12). Just upstream of SLVI is a structure-mapped 72-nt SL, SLV at nt 29 to 100 within the nsp1 cistron (genomic nt 239 to 310) (Fig. 2A) (12), whose function as a *cis*-acting higher-order structure has not yet been tested. To examine its potential *cis*-acting role in BCoV DI RNA replication, synonymous base substitutions designed to disrupt base pairings in a helical region and compensatory mutations designed to restore base pairings were tested. Silent helix-disrupting substitutions were feasible in only the downstream side of the bottom-most stem, for which changes U306C and U309C were made to form mutant pRt (where Rt and Lt refer to the right and left sides of the stems, respectively), and transcripts were tested for DI RNA replication. Following transfection into BCoV-infected cells, pRt DI RNA accumulation as determined by a visible band in Northern analysis was undetectable at 48 hpi and was present only at low levels in VP1 and VP2 compared to wt DI RNA levels (Fig. 2B). Sequence analysis of progeny RNA showed only wt revertants in VP2, indicating that the mutant had replicated poorly, if at all, and revertants with wt sequence, likely arising through recombination with the 5′ end of the helper virus genome, were selected (data not shown). However, when base pairings were restored by the compensatory mutations A240G and A243G in mutant pLtRt, replication as evidenced by accumulation of pLtRt DI RNA in Northern blots was restored to nearly wt levels in VP1 and VP2 (Fig. 2B), and mutations on both sides of the stem were retained in VP2 as revealed by sequence analysis (data not shown). A240G and A243G alone in mutant pLt were not predicted to disrupt base pairing in the stem, and, consistent with this structure, their presence alone did not block DI RNA replication, as evidenced by DI RNA accumulation in Northern blots (Fig. 2B) and sequence analysis. These results together indicate that optimal replication of DI RNA requires base pairing in the lowest helical region of SLV. Furthermore, when three silent point mutations were made in the upper loops of SLV, namely A264C, U273C, and G276A (Fig. 2A), to form the mutant named pLoops, the overall Mfold-predicted structure of SLV was only slightly changed (data not shown), and progeny DI RNA from pLoops, although slow in accumulating, retained the parent mutations in VP2. However, when the mutations in pLoops were combined with those in pRt to form pRt/Loops, there was additional structure disruption as predicted by Mfold, and accumulation was further impaired over pRt (Fig. 2B). That is, accumulation of pRt/Loops was not visible by Northern analysis at 48 hpi or in VP1 or VP2 (Fig. 2B) even though small amounts of wt progeny and progeny with reversions only at 306 and 309 were found by sequencing reverse transcription-PCR products (data not shown). These results

Downloaded from http://jvi.asm.org/ on March 29, 2015 by ST ANDREWS UNIV

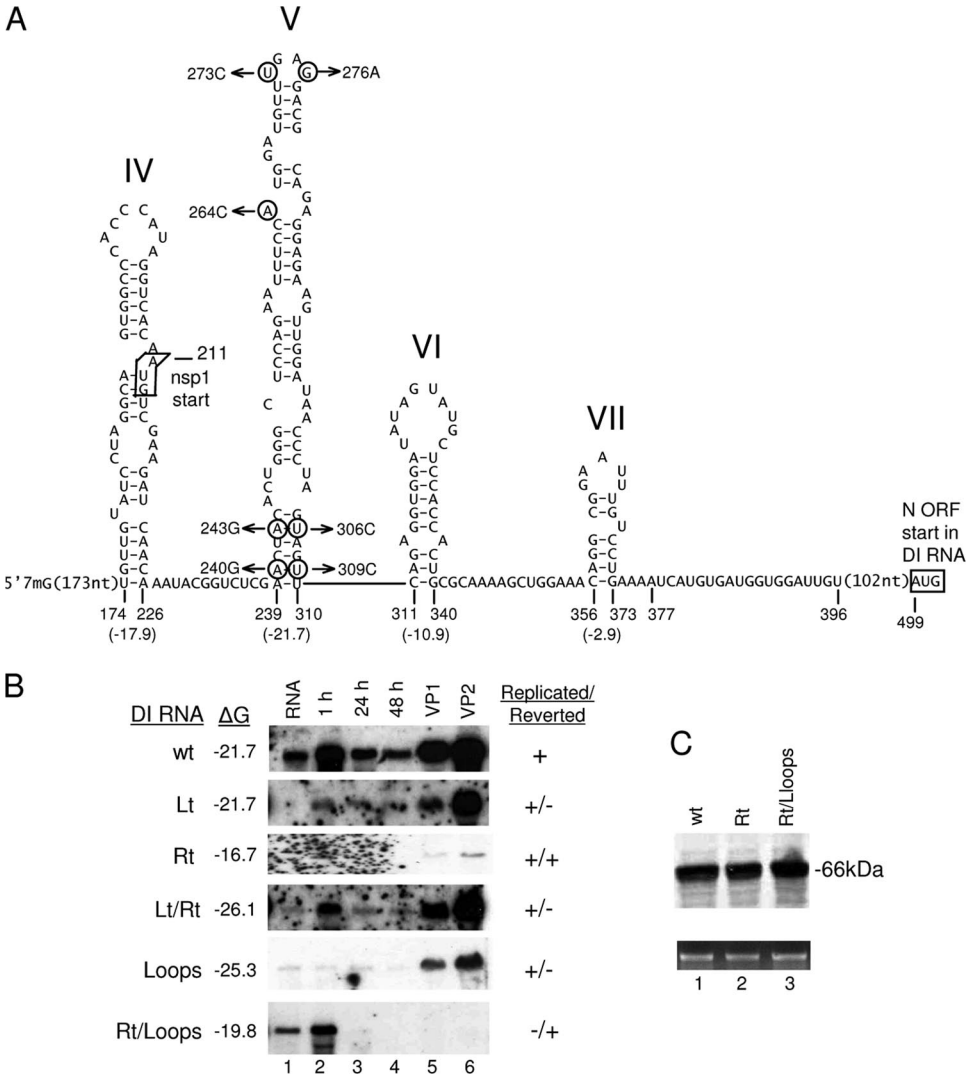

FIG. 2. Mutations in SLV that affect replication of wt BCoV DI RNA. (A) Mapped structures of SLIV-VI and predicted structure of SLVII in wt BCoV DI RNA (as found in pDrep1). Note that in mutant pΔ397–498 (12), nt 397 to 498 are deleted, which resulted in no loss of replicating ability. In mutant pΔ397–498 DI RNA, the N ORF begins at nt 397. The mutations in SLV are as follows: left, A240G and A243G; right, U306C and U309C; loops, A264C, U273C, and G276A; Rt/loops, U306C, U309C, A264C, U273C, and G276A. (B) Northern analysis of wt and SLV mutant DI RNAs. The calculated free energies (Δ*G*) of wt and mutated SLVs are shown. The Northern analyses used a ^{32}P-radiolabeled probe specific for the reporter sequence (30-nt TGEV reporter) on extracted RNA at the indicated times postinfection. RNA, a 1-ng sample of input RNA. Replication is based on the presence of DI RNA by Northern analysis in VP2, and reversion is judged from the sequence of the reverse transcription-PCR product in VP2 RNA. If only wt (i.e., reverted sequence) is found in VP2, the mutant is considered dead. (C) In vitro translation of wt and mutant DI RNA transcripts. The upper panel shows ^{35}S-radiolabeled translation product. The lower panel shows ethidium bromide-stained RNA transcript used for in vitro translation.

indicate that the overall higher-order structure of SLV, in addition to integrity in the lower stem, contributes to optimal BCoV DI RNA replication.

Translation of the partial 1a ORF has been shown to be a *cis* requirement for DI RNA replication (12, 14). To rule out the possibility that the observed loss of replication for SLV mutants was a result of unforeseen blocked translation arising from altered secondary structure (33), capped transcripts of wt and two selected mutants that did not replicate were translated in vitro in rabbit reticulocyte lysate, and the products were compared. Proteins translated in the presence of [^{35}S]methionine from equal amounts of RNA (Fig. 2C) were evaluated by SDS-PAGE, and the results showed that wt, pRt, and pRt/Loops translated at comparable levels (Fig. 2C). Thus, the observed decreases in RNA accumulation can be attributed to defects in RNA synthesis and not defects in translation.

Unidentified cellular proteins with molecular masses of ~60 and 100 kDa, but not nsp1, bind *cis*-acting SLV and SLVI. To test our hypothesis that nsp1 binds intra-nsp1 cistronic *cis*-replication elements SLV and SLVI, two approaches were taken. In the first, evidence of viral protein binding to the ^{32}P-labeled SLV-SLVI probe was sought by gel shift experiments with lysates of infected cells. In this analysis, three retarded proteinase K-sensitive complexes were found that were

Downloaded from http://jvi.asm.org/ on March 29, 2015 by ST ANDREWS UNIV

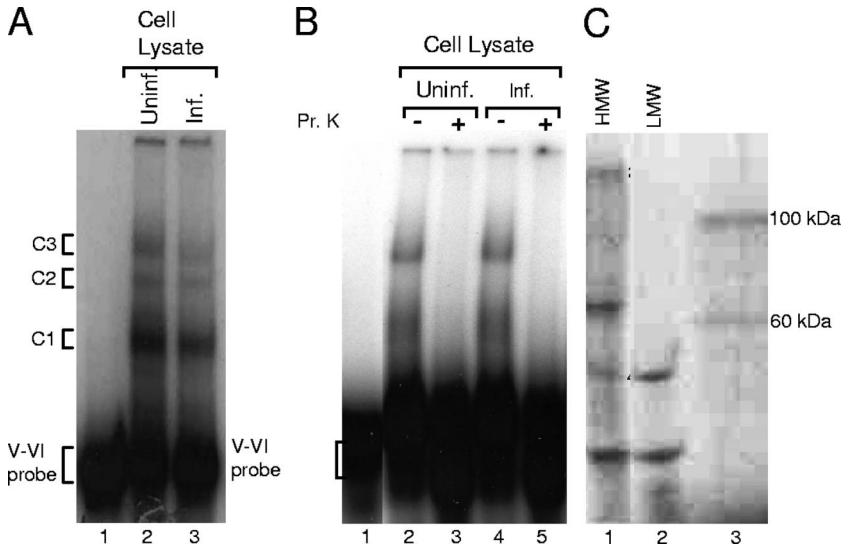

FIG. 3. Cellular proteins but apparently no viral proteins from cell lysates bind the SLV-VI probe. (A) Three gel shift complexes are formed with lysates of uninfected (Uninf) and infected (Inf) cells with SLV-VI probe. (B) Protein-RNA complexes with SLV-VI probe are destroyed by proteinase K (Pr K) treatment. (C) Proteins of 100 and 60 kDa from uninfected cell lysate UV cross-link to the SLV-VI probe. HMW, high-molecular-weight protein markers; LMW, low-molecular-weight protein markers.

also present with lysates from uninfected cells (Fig. 3A and B), suggesting that SLV and SLVI are bound by cellular but not viral proteins. The number and molecular masses of bound proteins were determined by UV cross-linking followed by RNase digestion and SDS-PAGE to be species with molecular masses of ~60 kDa and ~100 kDa (Fig. 3C). The identity of these and the significance of their interactions with SLV SLVI remain to be determined.

In the second approach, binding was sought with recombinant nsp1 from *E. coli*. When purified nsp1 was incubated with ^{32}P-labeled SLV-SLVI, SLV, SLVI, or (putative) SLVII probes, no gel shifting was observed although shifting was found with other terminal *cis*-acting structures noted below, indicating by this second method that nsp1 does not bind *cis*-acting SLV-VI (Fig. 1B).

nsp1 binds *cis*-replication structures in the 5′ and 3′ UTRs. Coronaviral proteins other than nsp1 have been shown to bind *cis*-replication structures: N protein binds the 5′-proximal SLII region (46, 61, 62), 2′-*O*-methyltransferase (nsp16) binds the 3′-terminal octamer-associated bulged stem-loop (A. Dziduszko et al., unpublished data), and an unknown viral protein(s) from infected cell lysates binds SLIII (S. Raman and D. Brian, unpublished data). Therefore, we systematically sought the binding of nsp1 to the three 5′ UTR-located *cis*-replication elements SLI-SLII, SLIII, and SLIV and two 3′ UTR-located *cis*-replication elements, the bulged SL-pseudoknot and the octamer-associated bulged SL. Binding of nsp1 to these would suggest other possible sites for nsp1 regulation of translation or RNA synthesis. In gel shift experiments, nsp1 was not found to bind the 3′ proximal bulged SL-pseudoknot but was found to weakly bind 5′-proximal SLI-SLII and SLIV, to moderately bind the 3′-terminal octamer-associated bulged SL, and to quantitatively shift the probe representing 5′ SLIII with its extended flanking sequences (sequences of 28 nt upstream and 67 nt downstream [SLIII-Long]) (Fig. 1B). Additionally, it was not found to bind the 5′-proximal uncharacterized putative SLVII in the partial nsp1 cistron (Fig. 1B). These results indicate that nsp1 is an RNA-binding protein that may function to regulate RNA translation or replication through its interaction with 5′ or 3′ *cis*-replication elements but not through binding to SLV-SLVI.

nsp1 binds SLIII and its flanking sequences with specificity and micromolar affinity. Since nsp1 caused a quantitative shift in the SLIII-Long probe, we sought to establish both its specificity and affinity of binding to SLIII-Long, as shown in Fig. 1, and SLIII-short (SLIII with flanking sequences of only 10 nt upstream and 10 nt downstream), which nearly represents SLIII proper. Figure 4A, lane 1, shows that the SLIII-Long probe migrates as upper and lower bands, probably representing two folded forms of the probe. Lane 2 shows approximately 50% of the lower form and all of the upper form of the probe fully shifting positions with 2.5 μM nsp1, indicating a K_d (dissociation constant) of ~2.5 μM for nsp1 binding to SLIII-Long. Figure 4A (lanes 5 to 7) shows a complete inhibition of SLIII-Long shifting with 5, 10, and 15 μg of unlabeled probe, representing 2,500, 5,000, and 7,500 molar excess over labeled probe, respectively, whereas no inhibition was seen with 5, 10, and 15 μg of tRNA. These results together show specific binding of nsp1 to SLIII-Long. Figure 4B, (lane 1) shows the SLIII-Short probe migrating as a single band. Lanes 2 to 4 show far less quantitative shifting of the probe to an upper band, and thus binding affinity was not determined by these experiments. Lanes 5 to 7, however, show that a band shifting with 2.5 μM protein was completely inhibited by the addition of 4, 8, and 12 μg, respectively, of unlabeled SLIII-Short probe, whereas lanes 8 to 10 show no inhibition of binding with 4, 8, and 12 μg of tRNA, respectively. These results show weaker but still specific binding of nsp1 to SLIII-Short. Together, the results show that whereas SLIII per se is probably a specific target for nsp1, the affinity of binding is greatly increased with the presence of its extended flanking sequences.

Downloaded from http://jvi.asm.org/ on March 29, 2015 by ST ANDREWS UNIV

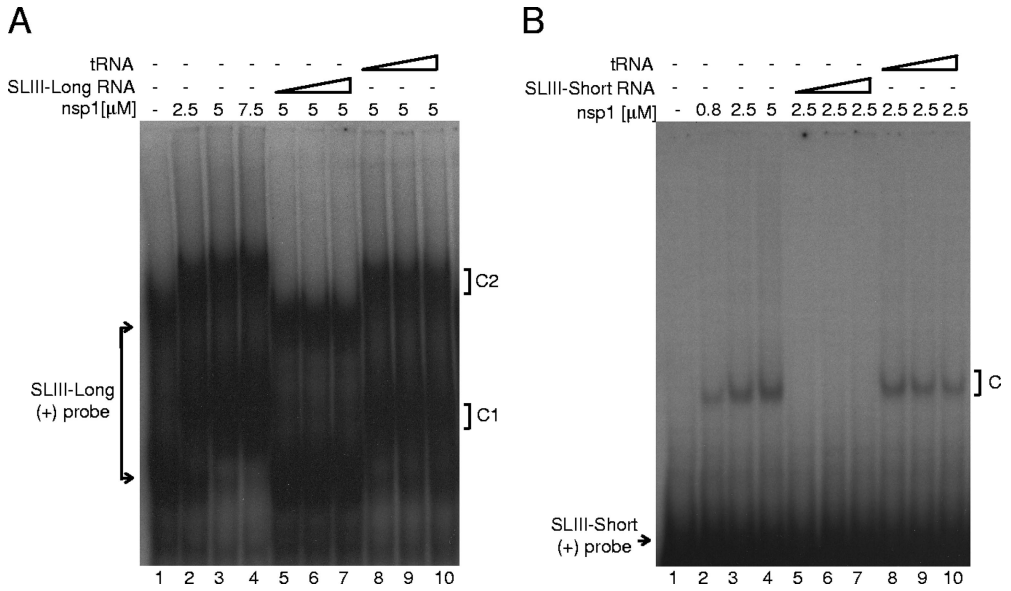

FIG. 4. Gel shift analysis of purified BCoV nsp1 binding to SLIII. (A) SLIII-Long. Lane 1, probe alone showing upper and lower forms; lanes 2 to 4, shifted bands into lower (C1) and upper (C2) complexes that form with the indicated amounts of protein; lanes 5 to 7, competition of protein binding with 5, 10, and 15 μg of unlabeled SLIII-Long RNA; lanes, 8 to 10, competition of protein binding with 5, 10, and 15 μg of tRNA over and above the tRNA in the binding buffer present in all lanes. (B) SLIII-Short. Lane 2, probe alone; lanes 2 to 4, shifted band with the indicated amounts of protein; lanes 5 to 7, competition of protein binding with 4, 8, and 12 μg of unlabeled SLIII-Short RNA; lanes 8 to 10, competition of protein binding with 4, 8, and 12 μg of tRNA over and above the tRNA in the binding buffer present in all lanes.

The nsp1 cistron positioned for sgmRNA expression from DI RNA leads to inhibition of DI RNA accumulation but to only slight transient inhibition of viral RNA. To determine whether higher than normal levels of nsp1 expression have an effect on BCoV replication, as might be expected of a regulatory protein, pDrep-ISnsp1 was constructed for testing; for this construct the BCoV nsp1 cistron was cloned into the BCoV DI RNA vector pDrepIS12.7 at a site known to express subgenomic RNA in 1.5-fold molar excess over viral genome when the intergenic transcription signaling sequence for the mRNA 7 (mRNA for N synthesis) is used (Fig. 5A) (75). Overexpression of a viral protein from a DI RNA would avoid a noncoronaviral expression system, and the expressed protein would presumably be available to the viral replication machinery within its membranous compartment (55, 67). When BCoV-infected cells were transfected with T7 RNA polymerase-generated DI RNA from pDrep12.7 (wt) (a DI RNA expressing a 116-aa fusion protein from the transcription start site of viral sgmRNA 5 [47, 75]) or pDrep-ΔISnsp1 (which is an nsp1 cistron-containing DI RNA construct missing the 18-nt IS transcription start signal) and evaluated by Northern analysis with a probe detecting the downstream reporter sequence (HSVgD), DI RNA progeny for each was observed through VP2 (Fig. 5B). These results indicate little or no inhibition of DI RNA replication. However, from infected cells transfected with pDrep-ISnsp1 RNA, no increase in DI RNA accumulation over input RNA was detected at 24 h posttransfection or beyond (Fig. 5B and C). Nor were sgmRNAs with the nsp1 cistron identified by Northern analysis at these times (data not shown) although they may have been present at earlier times posttransfection. In addition, no new bands were found that might have suggested recombination events between the DI RNAs and viral genome (data not shown). Therefore, direct evidence of nsp1 sgmRNA expression, as was shown for sgmRNA expression from pDrep12.7v(75), was not obtained. A blockage in the accumulation of DI RNA was not likely an effect of the nsp1 coding sequence within the DI RNA since the same sequence is present in pDrep-ΔISnsp1, which underwent replication. Interestingly, inhibition of DI RNA accumulation was observed not only with apparent expression of full-length nsp1 from a sgmRNA but also with expression of the C-terminal region of nsp1 from pDrep-ISnsp1$^{95\text{-}246}$ (genomic nt 493 to 948; nsp1 aa 95 to 246), representing a part of the genome whose homologous region in MHV can be deleted without loss of viral viability (Fig. 5B and C) (10). Less but still significant inhibition was seen with the N-terminal region of nsp1 from pDrep-ISnsp1$^{1\text{-}95}$ (genomic nt 211 to 495; nsp1 aa 1 to 95), a sequence whose homolog in the MHV nsp1 cistron contains a 30-nt sequence (nt 255 to 369) required for MHV genome replication (10, 21).

In addition, reduction in viral genome and sgmRNA levels with nsp1-expressing DI RNA was only slight and short-lived compared with expression levels in pDrep12.7-transfected cells (Fig. 5D to F). That is, a twofold reduction in viral sgmRNAs 6 and 7, the earliest appearing helper virus RNA species, was observed at 24 h posttransfection (Fig. 5E and F), but after this time wt levels were reached. No inhibition of viral genome or sgmRNAs was observed with expression of the C- and N-terminal regions of nsp1 (Fig. 5D to F).

We interpret these results together to mean that inhibitory levels of nsp1 were expressed from sgmRNA, although direct evidence for this expression remains to be shown, and that translation or replication of the DI RNA was more sensitive to the effects of nsp1 than that of viral genome or sgmRNAs. It is

Downloaded from http://jvi.asm.org/ on March 29, 2015 by ST ANDREWS UNIV

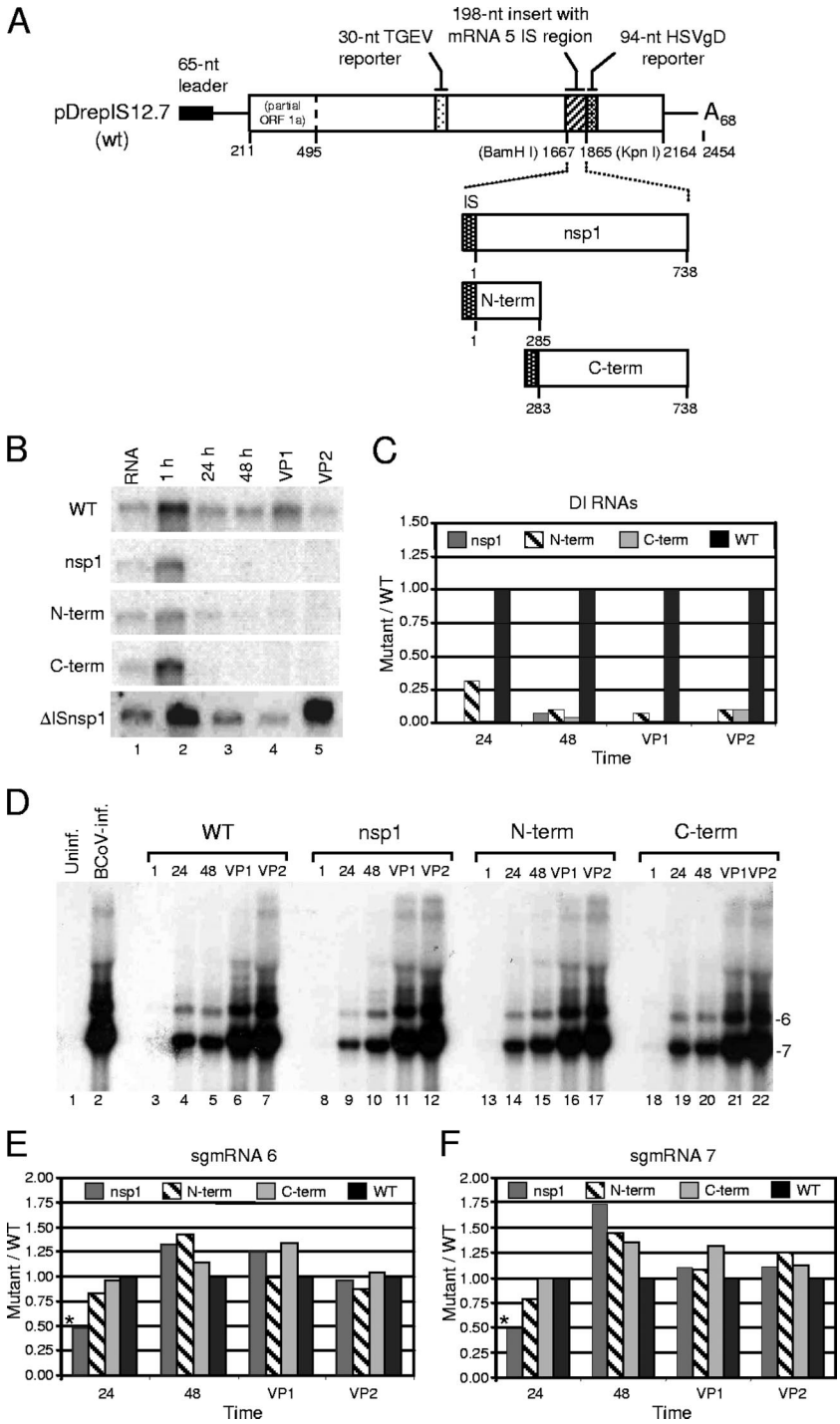

FIG. 5. Detrimental effects of nsp1 expression from subgenomic mRNA in DI RNA. (A) Map of DI RNA constructs for expressing the full-length nsp1, the N-terminal 95 aa (N-term; aa 1 to 95), and the C-terminal 152 aa (C-term; aa 95 to 246) of nsp1. The IS used to induce sgmRNA transcripts for nsp1 expression is the 18-nt sequence upstream of the BCoV N mRNA (sgmRNA 7) (see text). (B) Northern analysis of in vivo generated transcripts of wt and truncated nsp1 constructs shown in panel A as identified by a probe specific for DI RNA (HSVgD reporter). Results from control constructs are also shown. ΔISnsp1 represents a construct identical to pDrep-ISnsp1 except that the 18-nt IS is deleted. RNA, a 1-ng sample of input RNA. (C) Quantitative summary of PhosphorImager data collected from data in panel B. (D) Northern analysis of viral RNA probed with a 3′ end-specific probe [3′UTR(+)]. sgmRNAs 6 and 7 are identified. (E and F) Quantitative summary of phosphor imaging data shown in panel D for sgmRNA 6 and sgmRNA 7, respectively. Asterisks identify the most inhibited quantities of sgmRNA 6 and sgmRNA 7 observed with nsp1 expression from DI RNA. Uninf, uninfected; inf, infected.

Downloaded from http://jvi.asm.org/ on March 29, 2015 by ST ANDREWS UNIV

FIG. 6. Aligned amino acid sequences for nsp1 in BCoV (p28), MHV (p28), and SARS-CoV (p20). The arrowhead identifies the separation site of BCoV nsp1 into the N-terminal and C-terminal parts studied in the experiments shown in Fig. 5. The potential zinc finger-like RNA-binding domain in BCoV and MHV (nt 34 to 75) is identified by highlighting. Also highlighted (gray shading) in all three viruses is a highly similar 8-aa sequence in nsp1 (nt 192 to 199) that identifies a potential positively charged region of the protein. Numbers refer to amino acid positions in the BCoV sequence. Regions in the proteins coinciding with the coding regions harboring SLV and SLVI are indicated.

possible that as a transacting regulatory protein, nsp1 remains more localized in a DI-replicating compartment and does not freely diffuse to the replication-transcription complex of the viral genome.

DISCUSSION

Here, we test the hypothesis that nsp1 (p28) of BCoV, the first replicase protein to be synthesized and proteolytically released, is an RNA-binding protein that binds the *cis*-acting SLVI replication element within the nsp1 cistron. Binding of nsp1 to this structure would identify a potential means for autoregulation of gene expression. The rationale for this hypothesis is stated in the introduction. Although in this study we found no evidence of nsp1 binding to the intracistronic SLVI (12) as the hypothesis predicted, or to a newly identified SLV *cis*-acting replication signal immediately upstream of SLVI within the nsp1 cistron (this study), binding was found at other sites within the 5′ and 3′ UTRs that might function to regulate translation or replication. Notably, binding to a long form of *cis*-acting SLIII in the 5′ UTR with ~2.5 μM affinity was found.

To our knowledge, this is the first report of an RNA-binding property for CoV nsp1. While we tested binding here to only specific terminal regions of genomic RNA, the presence of multiple binding sites suggests possible broad-spectrum binding activity with other sites in the viral genome and also suggests relevance to the variety of cellular responses to CoV infection noted in several recent reports (16, 30, 45, 70, 79). Binding of nsp1 to cellular RNAs, for example, might induce pathogenic cellular responses. To date, however, only protein-protein interactions have been evaluated in these processes.

With regard to direct involvement of nsp1 in virus replication, several possibilities can be envisioned that will need testing. (i) nsp1 bound to SLIII (or SLs III and IV) might repress translation of ORF 1. The moderately high affinity of nsp1 for the long form of SLIII in the 5′ UTR and perhaps the lesser but still specific affinity to SLIV are consistent with results of an earlier study showing a 12-fold repression of translation in BCoV-infected cells for a reporter mRNA carrying the 210-nt genomic 5′ UTR but not one carrying the 77-nt 5′ UTR of sgmRNA 7 (54). That is, SLIII and SLIV are present in the 210-nt genomic 5′ UTR that experienced repression but not in the 77-nt sgmRNA 5′ UTR that experienced no repression (54). The molecules tested in these experiments had identical 3′ UTRs (54). If the observed repression is a function of a viral protein as postulated (54), then nsp1 becomes a candidate for this function. It is intriguing that SLIII contains some portion of a short upstream ORF found in virtually all CoV genomes (50). Although the function of the upstream ORF has yet to be found, conceivably it or its translated product plays a role in regulating translation or RNA replication, and nsp1 by binding SLIII may influence these processes. Based on precedents in other well-studied positive-strand RNA viruses, an inhibition of translation might facilitate negative-strand synthesis in a couple of ways. (a) nsp1 binding might block ribosomal transit and enable initiation of negative-strand synthesis. (b) nsp1 might interact with SLs I to IV and also the 3′ end, or other 3′ end-binding components, to form a circular molecule that functions to inhibit translation and enable initiation of negative-strand synthesis as has been shown for picornaviruses (5, 22). (ii) nsp1 might interact with a membrane-anchoring protein to bring the genome into the membrane-protected replication compartments, where the viral replication complex assembles and presumably functions in the absence (mostly) of the cellular translation machinery (55, 67). This mechanism, too, has precedence in nodaviruses and several plant viruses (68). (iii) nsp1 by binding directly to the very 3′ end of the genome might take part in replication complex formation and initiation of negative-strand synthesis. (iv) nsp1 through its affinity for SLIII in the 5′ UTR may play a role in RNA-dependent RNA polymerase template-switching events that direct leader formation at the 3′ end of sgmRNA-length templates for sgmRNA synthesis (74, 75). (v) Finally, nsp1 might function in the initiation of nascent positive strands from the 3′ end of the negative-strand antigenome. For this, a systematic study has not been made, but we have learned that SLIII does specifically, although weakly, bind the negative-strand counterparts to SLIII-Long and SLIII-Short (data not shown), suggesting a possible role for nsp1 in positive-strand synthesis.

At this time we have no experimental evidence to explain

Downloaded from http://jvi.asm.org/ on March 29, 2015 by ST ANDREWS UNIV

how expression of nsp1 from a DI RNA affects the accumulation of DI RNA more than that of helper virus genome and sgmRNAs, but it is possible that the DI RNA is simply more sensitive to nsp1 function or that it is in a different membranous compartment than the viral genome and sgmRNAs and therefore experiences a higher concentration of nsp1. The fact that both the N-terminal and C-terminal regions affect accumulation suggests that there is more than one functional domain within nsp1 involved in regulation. Nevertheless, a nearly complete repression of DI RNA accumulation and a twofold repression of viral sgmRNA abundance, even if short-lived, is suggestive evidence that nsp1 has an effect on viral mRNA expression.

Both the identity and function of the ~60- and 100-kDa cellular proteins that bind SLV-SLVI remain to be determined. Curiously, six cellular proteins with molecular masses of 25 to 58 kDa but no viral proteins were found to bind SLIV in the 5′ UTR (51). The arrangement of three *cis*-acting elements in close proximity suggests that they might function together as a larger structure. Although a relationship between cellular proteins binding SLV-SLVI or SLIV-SLVI and translation inhibition has not yet been shown, it is possible that the cellular proteins play a role in targeting the viral genome to the membranes making up the replication compartment (67).

Where is the RNA binding domain in nsp1? Bioinformatics analysis of the BCoV p28 amino acid sequence predicts no obvious RNA binding domain but does reveal a potential Zn finger with similarity to RNA binding motifs (13, 26). This domain (aa 34 to 75), common to both BCoV and MHV, is highlighted in Fig. 6. It has also been noted that an 8-amino-acid C-proximal domain of unknown function, also highlighted in Fig. 6, is conserved among all group 2 CoVs including the SARS-CoV, and the positively charged surface of this domain could be an RNA binding site (1). The functional RNA binding domain in nsp1, however, remains to be experimentally determined.

We conclude that, together, the results indicate that nsp1 is an RNA-binding protein that may function as a regulator of viral translation or replication but not through the binding of 5′-proximal *cis*-acting SLV and SLVI within its coding region. How and where nsp1 functions as an RNA-binding protein, and how SLV and SLVI function as *cis*-regulatory structures are questions that remain to be answered.

ACKNOWLEDGMENTS

We thank Kim Nixon and Hung-Yi Wu for many helpful discussions.

This work was supported by Public Health Service grant AI014367 from the National Institute of Allergy and Infectious Diseases and by funds from the University of Tennessee, College of Veterinary Medicine, Center of Excellence Program for Livestock Diseases and Human Health.

REFERENCES

1. **Almeida, M. S., M. A. Johnson, T. Herrmann, M. Geralt, and K. Wuthrich.** 2007. Novel β-barrel fold in the nuclear magnetic resonance structure of the replicase nonstructural protein 1 from the severe acute respiratory syndrome coronavirus. J. Virol. **81:**3151–3161.
2. **Andino, R., G. E. Rieckhof, and D. Baltimore.** 1990. A functional ribonucleoprotein complex forms around the 5′ end of poliovirus RNA. Cell **63:**369–380.
3. **Ball, L. A.** 2001. Replication strategies of RNA viruses, p. 105–118. *In* D. M. Knipe, P. M. Howley, D. E. Griffin, R. A. Lamb, M. A. Martin, B. Roizman, and S. E. Straus (ed.), Fields virology, 4th ed. Lippincott Williams & Wilkins, Philadelphia, PA.
4. **Barton, D. J., B. J. Morasco, and J. B. Flanegan.** 1999. Translating ribosomes inhibit poliovirus negative-strand RNA synthesis. J. Virol. **73:**10104–10112.
5. **Barton, D. J., B. J. O'Donnell, and J. B. Flanegan.** 2001. 5′ Cloverleaf in poliovirus RNA is a cis-acting replication element required for negative-strand synthesis. EMBO J. **20:**1439–1448.
6. **Bhardwaj, K., S. Palaninathan, J. M. Alcantara, L. L. Yi, L. Guarino, J. C. Sacchettini, and C. C. Kao.** 2008. Structural and functional analyses of the severe acute respiratory syndrome coronavirus endoribonuclease Nsp15. J. Biol. Chem. **283:**3655–3664.
7. **Brian, D. A., and Spaan, W. J. M.** 1997. Recombination and coronavirus defective interfering RNAs. Sem. Virol. **8:**101–111.
8. **Brian, D. A., and R. S. Baric.** 2005. Coronavirus genome structure and replication. Curr. Top. Microbiol. Immunol. **287:**1–30.
9. **Brierley, I., M. E. Boursnell, M. M. Binns, B. Bilimoria, V. C. Blok, T. D. Brown, and S. C. Inglis.** 1987. An efficient ribosomal frame-shifting signal in the polymerase-encoding region of the coronavirus IBV. EMBO J. **6:**3779–3785.
10. **Brockway, S. M., and M. R. Denison.** 2005. Mutagenesis of the murine hepatitis virus nsp1-coding region identifies residues important for protein processing, viral RNA synthesis, and viral replication. Virology **340:**209–223.
11. **Brockway, S. M., X. T. Lu, T. R. Peters, T. S. Dermody, and M. R. Denison.** 2004. Intracellular localization and protein interactions of the gene 1 protein p28 during mouse hepatitis virus replication. J. Virol. **78:**11551–11562.
12. **Brown, C. G., K. S. Nixon, S. D. Senanayake, and D. A. Brian.** 2007. An RNA stem-loop within the bovine coronavirus nsp1 coding region is a *cis*-acting element in defective interfering RNA replication. J. Virol. **81:**7716–7724.
13. **Brown, R. S.** 2005. Zinc finger proteins: getting a grip on RNA. Curr. Opin. Struct. Biol. **15:**94–98.
14. **Chang, R. Y., and D. A. Brian.** 1996. cis Requirement for N-specific protein sequence in bovine coronavirus defective interfering RNA replication. J. Virol. **70:**2201–2207.
15. **Chang, R. Y., M. A. Hofmann, P. B. Sethna, and D. A. Brian.** 1994. A cis-acting function for the coronavirus leader in defective interfering RNA replication. J. Virol. **68:**8223–8231.
16. **Chen, C. J., K. Sugiyama, H. Kubo, C. Huang, and S. Makino.** 2004. Murine coronavirus nonstructural protein p28 arrests cell cycle in G_0/G_1 phase. J. Virol. **78:**10410–10419.
17. **Decroly, E., I. Imbert, B. Coutard, M. Bouvet, B. Selisko, K. Alvarez, A. E. Gorbalenya, E. J. Snijder, and B. Canard.** 2008. Coronavirus nonstructural protein 16 is a cap-0 binding enzyme possessing (nucleoside-2′*O*)-methyltransferase activity. J. Virol. **82:**8071–8084.
18. **Denison, M., and S. Perlman.** 1987. Identification of putative polymerase gene product in cells infected with murine coronavirus A59. Virology **157:**565–568.
19. **Donaldson, E. F., R. L. Graham, A. C. Sims, M. R. Denison, and R. S. Baric.** 2007. Analysis of murine hepatitis virus strain A59 temperature-sensitive mutant TS-LA6 suggests that nsp10 plays a critical role in polyprotein processing. J. Virol. **81:**7086–7098.
20. **Donaldson, E. F., A. C. Sims, R. L. Graham, M. R. Denison, and R. S. Baric.** 2007. Murine hepatitis virus replicase protein nsp10 is a critical regulator of viral RNA synthesis. J. Virol. **81:**6356–6368.
21. **Eckerle, L. D., S. M. Brockway, S. M. Sperry, X. Lu, and M. R. Denison.** 2006. Effects of mutagenesis of murine hepatitis virus nsp1 and nsp14 on replication in culture. Adv. Exp. Med. Biol. **581:**55–60.
22. **Gamarnik, A. V., and R. Andino.** 1998. Switch from translation to RNA replication in a positive-stranded RNA virus. Genes Dev. **12:**2293–2304.
23. **Goebel, S. J., B. Hsue, T. F. Dombrowski, and P. S. Masters.** 2004. Characterization of the RNA components of a putative molecular switch in the 3′ untranslated region of the murine coronavirus genome. J. Virol. **78:**669–682.
24. **Gorbalenya, A. E., L. Enjuanes, J. Ziebuhr, and E. J. Snijder.** 2006. *Nidovirales*: evolving the largest RNA virus genome. Virus Res. **117:**17–37.
25. **Graham, R. L., A. C. Sims, R. S. Baric, and M. R. Denison.** 2006. The nsp2 proteins of mouse hepatitis virus and SARS coronavirus are dispensable for viral replication. Adv. Exp. Med. Biol. **581:**67–72.
26. **Hall, T. M.** 2005. Multiple modes of RNA recognition by zinc finger proteins. Curr. Opin. Struct. Biol. **15:**367–373.
27. **Hsue, B., T. Hartshorne, and P. S. Masters.** 2000. Characterization of an essential RNA secondary structure in the 3′ untranslated region of the murine coronavirus genome. J. Virol. **74:**6911–6921.
28. **Hsue, B., and P. S. Masters.** 1997. A bulged stem-loop structure in the 3′ untranslated region of the genome of the coronavirus mouse hepatitis virus is essential for replication. J. Virol. **71:**7567–7578.
29. **Imbert, I., J. C. Guillemot, J. M. Bourhis, C. Bussetta, B. Coutard, M. P. Egloff, F. Ferron, A. E. Gorbalenya, and B. Canard.** 2006. A second, non-canonical RNA-dependent RNA polymerase in SARS coronavirus. EMBO J. **25:**4933–4942.
30. **Kamitani, W., K. Narayanan, C. Huang, K. Lokugamage, T. Ikegami, N. Ito, H. Kubo, and S. Makino.** 2006. Severe acute respiratory syndrome coronavirus nsp1 protein suppresses host gene expression by promoting host mRNA degradation. Proc. Natl. Acad. Sci. USA **103:**12885–12890.
31. **Kolakofsky, D., and C. Weissmann.** 1971. Possible mechanism for transition of viral RNA from polysome to replication complex. Nat. New Biol. **231:**42–46.

Downloaded from http://jvi.asm.org/ on March 29, 2015 by ST ANDREWS UNIV

32. **Kolakofsky, D., and C. Weissmann.** 1971. Q. replicase as repressor of Q. RNA-directed protein synthesis. Biochim. Biophys. Acta **246:**596–599.
33. **Kozak, M.** 1991. Structural features in eukaryotic mRNAs that modulate the initiation of translation. J. Biol. Chem. **266:**19867–19870.
34. **Krishnan, R., R. Y. Chang, and D. A. Brian.** 1996. Tandem placement of a coronavirus promoter results in enhanced mRNA synthesis from the downstream-most initiation site. Virology **218:**400–405.
35. **Lai, M. C., and K. V. Holmes.** 2001. Coronaviridae: The Viruses and Their Replication, p. 1163–1186. *In* D. M. Knipe, P. M. Howley, D. E. Griffin, R. A. Lamb, M. A. Martin, B. Roizman, and S. E. Straus (ed.), Fields virology, vol. 1, 4th ed. Lippincott Williams & Wilkins, Philadelphia, PA.
36. **Law, A. H., D. C. Lee, B. K. Cheung, H. C. Yim, and A. S. Lau.** 2007. Role for nonstructural protein 1 of severe acute respiratory syndrome coronavirus in chemokine dysregulation. J. Virol. **81:**416–422.
37. **Letunic, I., R. R. Copley, B. Pils, S. Pinkert, J. Schultz, and P. Bork.** 2006. SMART 5: domains in the context of genomes and networks. Nucleic Acids Res. **34:**D257–D260.
38. **Liu, P., L. Li, J. J. Millership, H. Kang, J. L. Leibowitz, and D. P. Giedroc.** 2007. A U-turn motif-containing stem-loop in the coronavirus 5′ untranslated region plays a functional role in replication. RNA **13:**763–780.
39. **Liu, Q., R. F. Johnson, and J. L. Leibowitz.** 2001. Secondary structural elements within the 3′ untranslated region of mouse hepatitis virus strain JHM genomic RNA. J. Virol. **75:**12105–12113.
40. **Marra, M. A., S. J. Jones, C. R. Astell, R. A. Holt, A. Brooks-Wilson, Y. S. Butterfield, J. Khattra, J. K. Asano, S. A. Barber, S. Y. Chan, A. Cloutier, S. M. Coughlin, D. Freeman, N. Girn, O. L. Griffith, S. R. Leach, M. Mayo, H. McDonald, S. B. Montgomery, P. K. Pandoh, A. S. Petrescu, A. G. Robertson, J. E. Schein, A. Siddiqui, D. E. Smailus, J. M. Stott, G. S. Yang, F. Plummer, A. Andonov, H. Artsob, N. Bastien, K. Bernard, T. F. Booth, D. Bowness, M. Czub, M. Drebot, L. Fernando, R. Flick, M. Garbutt, M. Gray, A. Grolla, S. Jones, H. Feldmann, A. Meyers, A. Kabani, Y. Li, S. Normand, U. Stroher, G. A. Tipples, S. Tyler, R. Vogrig, D. Ward, B. Watson, R. C. Brunham, M. Krajden, M. Petric, D. M. Skowronski, C. Upton, and R. L. Roper.** 2003. The genome sequence of the SARS-associated coronavirus. Science **300:**1399–1404.
41. **Masters, P. S.** 2006. The molecular biology of coronaviruses. Adv. Virus Res. **66:**193–292.
42. **Mathews, D. H., J. Sabina, M. Zuker, and D. H. Turner.** 1999. Expanded sequence dependence of thermodynamic parameters improves prediction of RNA secondary structure. J. Mol. Biol. **288:**911–940.
43. **Matthes, N., J. R. Mesters, B. Coutard, B. Canard, E. J. Snijder, R. Moll, and R. Hilgenfeld.** 2006. The non-structural protein Nsp10 of mouse hepatitis virus binds zinc ions and nucleic acids. FEBS Lett. **580:**4143–4149.
44. **Minskaia, E., T. Hertzig, A. E. Gorbalenya, V. Campanacci, C. Cambillau, B. Canard, and J. Ziebuhr.** 2006. Discovery of an RNA virus 3′→5′ exoribonuclease that is critically involved in coronavirus RNA synthesis. Proc. Natl. Acad. Sci. USA **103:**5108–5113.
45. **Narayanan, K., C. Huang, K. Lokugamage, W. Kamitani, T. Ikegami, C. T. Tseng, and S. Makino.** 2008. Severe acute respiratory syndrome coronavirus nsp1 suppresses host gene expression, including that of type I interferon, in infected cells. J. Virol. **82:**4471–4479.
46. **Nelson, G. W., and S. A. Stohlman.** 1993. Localization of the RNA-binding domain of mouse hepatitis virus nucleocapsid protein. J. Gen. Virol. **74:** 1975–1979.
47. **Ozdarendeli, A., S. Ku, S. Rochat, G. D. Williams, S. D. Senanayake, and D. A. Brian.** 2001. Downstream sequences influence the choice between a naturally occurring noncanonical and closely positioned upstream canonical heptameric fusion motif during bovine coronavirus subgenomic mRNA synthesis. J. Virol. **75:**7362–7374.
48. **Pestova, T. V., C. U. Hellen, and E. Wimmer.** 1991. Translation of poliovirus RNA: role of an essential cis-acting oligopyrimidine element within the 5′ nontranslated region and involvement of a cellular 57-kilodalton protein. J. Virol. **65:**6194–6204.
49. **Ponnusamy, R., R. Moll, T. Weimar, J. R. Mesters, and R. Hilgenfeld.** 2008. Variable oligomerization modes in coronavirus non-structural protein 9. J. Mol. Biol. **383:**1081–1096.
50. **Raman, S., P. Bouma, G. D. Williams, and D. A. Brian.** 2003. Stem-loop III in the 5′ untranslated region is a *cis*-acting element in bovine coronavirus defective interfering RNA replication. J. Virol. **77:**6720–6730.
51. **Raman, S., and D. A. Brian.** 2005. Stem-loop IV in the 5′ untranslated region is a *cis*-acting element in bovine coronavirus defective interfering RNA replication. J. Virol. **79:**12434–12446.
52. **Sambrook, J., E. F. Fritsch, and T. Maniatis.** 1989. Molecular cloning: a laboratory manual, 2nd ed. Cold Spring Harbor Press, Cold Spring Harbor, NY.
53. **Schultz, J., F. Milpetz, P. Bork, and C. P. Ponting.** 1998. SMART, a simple modular architecture research tool: identification of signaling domains. Proc. Natl. Acad. Sci. USA **95:**5857–5864.
54. **Senanayake, S. D., and D. A. Brian.** 1999. Translation from the 5′ untranslated region (UTR) of mRNA 1 is repressed, but that from the 5′ UTR of mRNA 7 is stimulated in coronavirus-infected cells. J. Virol. **73:**8003–8009.
55. **Sethna, P. B., and D. A. Brian.** 1997. Coronavirus genomic and subgenomic minus-strand RNAs copartition in membrane-protected replication complexes. J. Virol. **71:**7744–7749.
56. **Sethna, P. B., S. L. Hung, and D. A. Brian.** 1989. Coronavirus subgenomic minus-strand RNAs and the potential for mRNA replicons. Proc. Natl. Acad. Sci. USA **86:**5626–5630.
57. **Silvera, D., A. V. Gamarnik, and R. Andino.** 1999. The N-terminal K homology domain of the poly(rC)-binding protein is a major determinant for binding to the poliovirus 5′-untranslated region and acts as an inhibitor of viral translation. J. Biol. Chem. **274:**38163–38170.
58. **Snijder, E. J., P. J. Bredenbeek, J. C. Dobbe, V. Thiel, J. Ziebuhr, L. L. Poon, Y. Guan, M. Rozanov, W. J. Spaan, and A. E. Gorbalenya.** 2003. Unique and conserved features of genome and proteome of SARS-coronavirus, an early split-off from the coronavirus group 2 lineage. J. Mol. Biol. **331:**991–1004.
59. **Spaan, W. J. M., D. Brian, D. Cavanagh, R. J. de Groot, L. Enjuanes, A. E. Gorbalenya, K. V. Holmes, P. Masters, P. Rottier, F. Taguchi, and P. Talbot.** 2005. *Coronaviridae*, p. 1259. *In* C. Fauquet, M. A. Mayo, J. Maniloff, U. Desselberger, and L. A. Ball (ed.), Virus taxonomy. Eighth report of the International Committee on Taxonomy of Viruses classification and nomenclature of viruses. Elsevier/Academic Press, San Diego, CA.
60. **Spagnolo, J. F., and B. G. Hogue.** 2000. Host protein interactions with the 3′ end of bovine coronavirus RNA and the requirement of the poly(A) tail for coronavirus defective genome replication. J. Virol. **74:**5053–5065.
61. **Stohlman, S. A., R. S. Baric, G. N. Nelson, L. H. Soe, L. M. Welter, and R. J. Deans.** 1988. Specific interaction between coronavirus leader RNA and nucleocapsid protein. J. Virol. **62:**4288–4295.
62. **Tahara, S. M., T. A. Dietlin, C. C. Bergmann, G. W. Nelson, S. Kyuwa, R. P. Anthony, and S. A. Stohlman.** 1994. Coronavirus translational regulation: leader affects mRNA efficiency. Virology **202:**621–630.
63. **Thomson, A. M., J. T. Rogers, C. E. Walker, J. M. Staton, and P. J. Leedman.** 1999. Optimized RNA gel-shift and UV cross-linking assays for characterization of cytoplasmic RNA-protein interactions. BioTechniques **27:**1032–1039, 1042.
64. **Tompkins, W. A., A. M. Watrach, J. D. Schmale, R. M. Schultz, and J. A. Harris.** 1974. Cultural and antigenic properties of newly established cell strains derived from adenocarcinomas of the human colon and rectum. J. Natl. Cancer Inst. **52:**1101–1110.
65. **van der Hoek, L., K. Pyrc, M. F. Jebbink, W. Vermeulen-Oost, R. J. Berkhout, K. C. Wolthers, P. M. Wertheim-van Dillen, J. Kaandorp, J. Spaargaren, and B. Berkhout.** 2004. Identification of a new human coronavirus. Nat. Med. **10:**368–373.
66. **van der Meer, Y., E. J. Snijder, J. C. Dobbe, S. Schleich, M. R. Denison, W. J. Spaan, and J. K. Locker.** 1999. Localization of mouse hepatitis virus nonstructural proteins and RNA synthesis indicates a role for late endosomes in viral replication. J. Virol. **73:**7641–7657.
67. **van Hemert, M. J., S. H. van den Worm, K. Knoops, A. M. Mommaas, A. E. Gorbalenya, and E. J. Snijder.** 2008. SARS-coronavirus replication/transcription complexes are membrane-protected and need a host factor for activity in vitro. PLoS Pathog **4:**e1000054.
68. **Van Wynsberghe, P. M., H. R. Chen, and P. Ahlquist.** 2007. Nodavirus RNA replication protein a induces membrane association of genomic RNA. J. Virol. **81:**4633–4644.
69. **Wang, J. T., and S. C. Chang.** 2004. Severe acute respiratory syndrome. Curr. Opin. Infect. Dis. **17:**143–148.
70. **Wathelet, M. G., M. Orr, M. B. Frieman, and R. S. Baric.** 2007. Severe acute respiratory syndrome coronavirus evades antiviral signaling: role of nsp1 and rational design of an attenuated strain. J. Virol. **81:**11620–11633.
71. **Weiss, S. R., and S. Navas-Martin.** 2005. Coronavirus pathogenesis and the emerging pathogen severe acute respiratory syndrome coronavirus. Microbiol. Mol. Biol. Rev. **69:**635–664.
72. **Williams, G. D., R. Y. Chang, and D. A. Brian.** 1999. A phylogenetically conserved hairpin-type 3′ untranslated region pseudoknot functions in coronavirus RNA replication. J. Virol. **73:**8349–8355.
73. **Woo, P. C., S. K. Lau, C. M. Chu, K. H. Chan, H. W. Tsoi, Y. Huang, B. H. Wong, R. W. Poon, J. J. Cai, W. K. Luk, L. L. Poon, S. S. Wong, Y. Guan, J. S. Peiris, and K. Y. Yuen.** 2005. Characterization and complete genome sequence of a novel coronavirus, coronavirus HKU1, from patients with pneumonia. J. Virol. **79:**884–895.
74. **Wu, H. Y., and D. A. Brian.** 2007. 5′-Proximal hot spot for an inducible positive-to-negative-strand template switch by coronavirus RNA-dependent RNA polymerase. J. Virol. **81:**3206–3215.
75. **Wu, H. Y., A. Ozdarendeli, and D. A. Brian.** 2006. Bovine coronavirus 5′-proximal genomic acceptor hotspot for discontinuous transcription is 65 nucleotides wide. J. Virol. **80:**2183–2193.
76. **Yu, W., and J. L. Leibowitz.** 1995. A conserved motif at the 3′ end of mouse hepatitis virus genomic RNA required for host protein binding and viral RNA replication. Virology **214:**128–138.
77. **Ziebuhr, J., E. J. Snijder, and A. E. Gorbalenya.** 2000. Virus-encoded proteinases and proteolytic processing in the *Nidovirales*. J. Gen. Virol. **81:**853–879.
78. **Zuker, M.** 2003. Mfold web server for nucleic acid folding and hybridization prediction. Nucleic Acids Res. **31:**3406–3415.
79. **Zust, R., L. Cervantes-Barragan, T. Kuri, G. Blakqori, F. Weber, B. Ludewig, and V. Thiel.** 2007. Coronavirus nonstructural protein 1 is a major pathogenicity factor: implications for the rational design of coronavirus vaccines. PLoS Pathog. **3:**e109.

Downloaded from http://jvi.asm.org/ on March 29, 2015 by ST ANDREWS UNIV